Development of Alkali-Activated Binders from Recycled Mixed Masonry-originated Waste

Gürkan Yıldırım[1*], Anıl Kul[2], Emircan Özçelikci[2], Mustafa Şahmaran[2], Alper Aldemir[2], Diogo Figueira[3], Ashraf Ashour[3]

[1] Department of Civil Engineering, Kırıkkale University, Kırıkkale, Turkey

[2] Department of Civil Engineering, Hacettepe University, Ankara, Turkey

[3] Department of Civil and Structural Engineering, University of Bradford, Bradford, United Kingdom

Abstract

In this study, the main emphasis is placed on the development and characterization of alkali-activated binders completely produced by the use of mixed construction and demolition waste (CDW)-based masonry units as aluminosilicate precursors. Combined usage of precursors was aimed to better simulate the real-life cases since in the incident of construction and demolition, these wastes are anticipated to be generated collectively. As different masonry units, red clay brick (RCB), hollow brick (HB) and roof tile (RT) were used in binary combinations by 75-25%, 50-50% and 25-75% of the total weight of the binder. Mixtures were produced with different curing temperature/periods and molarities of NaOH solution as the alkaline activator. Characterization was made by the compressive strength measurements supported by microstructural investigations which included the analyses of X-ray diffraction (XRD) and scanning electron microscopy with energy-dispersive X-ray spectroscopy (SEM/EDX). Results clearly showed that completely CDW-based masonry units can be effectively used collectively in producing alkali-activated binders having up to 80 MPa compressive strength provided that the mixture design parameters are optimized. Among different precursors utilized, HB seems to contribute more to the compressive strength. Irrespective of their composition, main reaction products of alkali-activated binders from CDW-based masonry units are sodium aluminosilicate hydrate (N-A-S-H) gels containing different zeolitic polytypes with structure ranging from amorphous to polycrystalline.

***Keywords*:** Alkali-activated materials (AAMs); Construction and demolition waste (CDW); Masonry, Compressive strength; Microstructure.

1. Introduction

Concrete is the most widely used construction material owing to its low cost, ease of applicability, versatility and reliability with yearly consumption levels approaching 30 billion tonnes [1]. As the developing countries invest more and more in their infrastructural development and developed countries upgrade/replace their ageing infrastructure, the demand for concrete increases continuously [1]. However, concrete production is not at a low cost given the fact that majority of the individual constituents forming this material is not eco-friendly and sustainable to manufacture. The most distinctive example of such constituents is Portland cement (PC) which is the main binder for traditional concrete and requires highly energy-intensive stages of production (e.g. fuel combustion and calcination of raw materials) resulting in release of nearly 1 ton of CO_2 per 1 ton of PC manufactured [2]. Currently, PC production is hold responsible for up to 9% of global anthropogenic CO_2 emissions and it is estimated that by 2050, annual PC production will increase by 50% [1]. In this sense, nowadays, the focus of research community is shifting towards the utilization of more eco-friendly binders in concrete.

Traditional concrete is reported to be not long-lived due to its brittle nature which triggers high cracking tendency and exacerbation of problems related to durability [3-6]. The insufficiency in the durability performance of conventional concrete which is coupled with the lack of control over cracking generally ends up with costly repair and/or maintenance applications [7] or even with the complete demolition and re-construction of structures, creating large amounts of waste collectively termed as "*Construction and Demolition Waste – CDW"*. CDW industry is regarded to be one of the sectors contributing to the global solid waste production the most [8]. Annual CDW production of major countries is ten billion tons. Three billion of this is contributed by China [9] while, EU-28 and U.S. generate more than 800 and

700 million tons, respectively [8]. As exemplified, CDW is a global issue requiring relatively high demand for proper handling. This is not only important to lower the CDW amount going to clean landfills, but also to reduce the amount of concrete (hence, PC and aggregates) production that is, otherwise, going to be used for the construction and repair/maintenance of new and/or existing structures.

Due to concerns about the tremendous amounts of concrete and related PC production worldwide, latest research efforts into the development of more eco-friendly binders have been intensified.

In this regard, "alkali-activated materials (AAMs)", including those referred to as "geopolymers" can be regarded as a major advancement towards the realization of greener binders [10]. AAMs can be synthesised by the alkali-activation of a variety of aluminosilicate precursors (source materials) and the majority of the studies up to now were performed using precursors such as fly ash, ground granulated blast furnace slag, silica fume and metakaolin. These precursors are already well-known and have controlled production processes and chemical compositions [11]. However, it is notable that these materials are highly demanded and very successfully utilized in blended PC production and as separate mineral admixtures in concrete mixtures. This therefore pushes researchers all around the world to look for possible aluminosilicate precursors that can be used in the production of AAMs instead of abovementioned main-stream mineral admixtures [12]. In this sense, CDW-based components such as waste concrete, glass, masonry (e.g. bricks, tiles, ceramic) can be regarded as valuable candidates and used as precursors in alkali-activation process which may favour more effective waste management/control and pave the way for novel routes of waste recycling.

Studies related to the production of alkali-activated binders with CDW-based precursors have already started although they are significantly limited in number and mostly utilized these precursors singly or in combination with the previously mentioned main-stream precursors to

control the overall performance of the ultimate material [13-19]. In the incidents of construction and demolition, CDW-based materials are obtained altogether. In order to obtain CDW-based components separately, selective construction and demolition practises need to be employed which may be energy-inefficient and time-consuming. It is therefore much more desirable to use CDW-based precursors simultaneously in the production of alkali-activated binders without elaborative separation to better simulate the first-hand obtained materials. To make an effort in this direction, here, it was aimed to produce and evaluate alkali-activated binders based on mixed CDW-based masonry units different from studies available in the literature. Red clay brick (RCB), hollow brick (HB) and roof tile (RT) were used in this study as different masonry units and in binary combinations by 75-25%, 50-50% and 25-75% of the total weight of the binder. While producing the alkali-activated binders, special attention was paid to curing of specimens produced with different alkaline activator concentrations and cured under different temperature/periods. Performance characterization of alkali-activated binders was made via series of compressive strength measurements which were backed by more in-depth microstructural analyses of X-ray diffraction (XRD) and scanning electron microscopy with energy-dispersive X-ray spectroscopy (SEM/EDX).

2. Experimental Program

2.1 Materials

In this study, CDW-based masonry units which include red clay brick (RCB), hollow brick (HB) and roof tile (RT) were used as obtained from an urban transformation area located in Ankara, Turkey. These materials were subjected to a non-complex, two-step, crushing-grinding procedure. The first step of the procedure consisted of loading the CDW-based materials into a laboratory-type jaw crusher which provided initial size reduction, followed by the second step which included the loading of the crushed materials into a ball mill and further grinding for an hour. In Fig. 1, views of CDW-based masonry units taken with the help of video camera and

scanning electron microscope (SEM) were shown. In Fig. 2, gradation curves which give information about the particle size distributions of the precursors were displayed. Characteristic particle diameters of precursors were shown in Table 1.

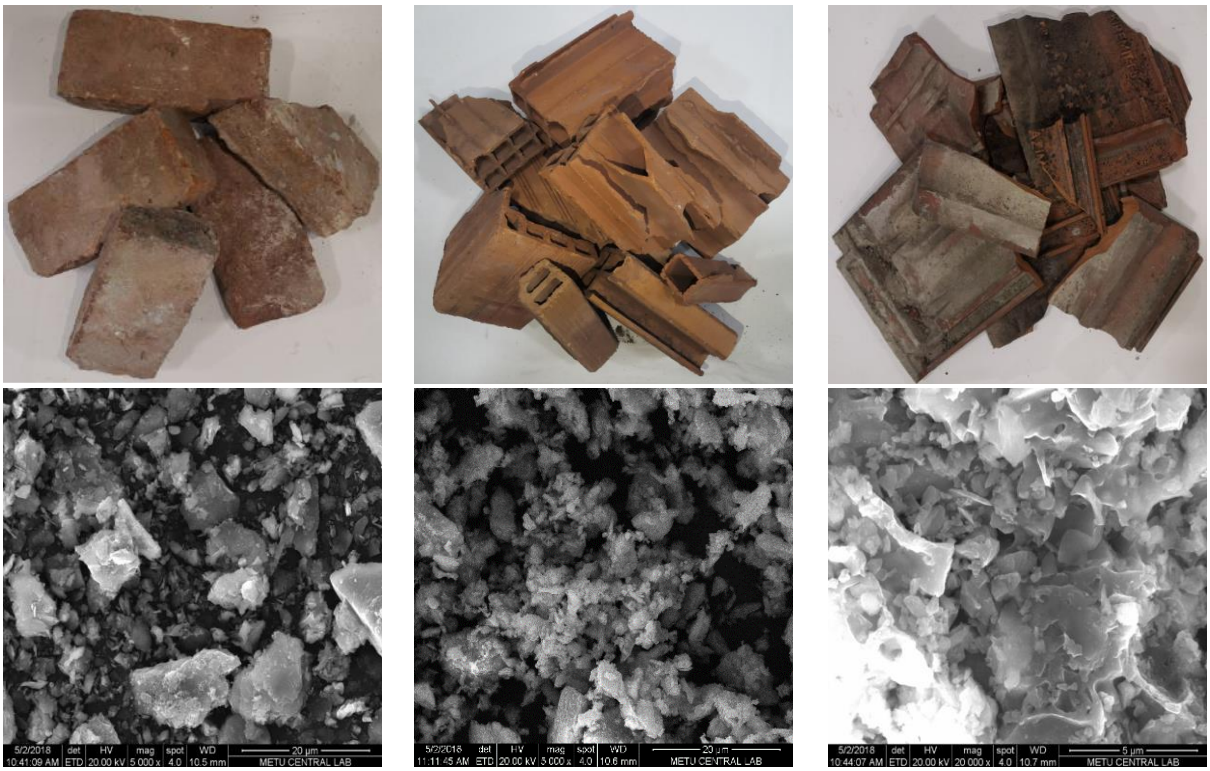

(a) (b) (c)

Fig. 1. Video camera and SEM views of CDW-based precursors (a) red clay brick (RCB), (b) hollow brick (HB), (c) roof tile (RT).

As can be seen from both Fig. 2 and Table 1, RCB is the finest CDW-based precursor followed by RT and HB. According to Komnitsas et al. [13], significant improvements can be achieved in the compressive strength of alkali-activated binders when fractions with $D_{50} < 15$ μm are used. However, only RCB was found to have a D_{50} value less than 15 μm (see Table 1). Further grinding to reach finer particle fractions for precursors was not intended in this study, since further milling is more labourious and energy-intensive. Another reason for the avoidance of further grinding of the precursors is related to more realistic simulation of the situation in practice. Upon construction/demolition of a certain structure, different waste types are obtained

collectively and it is therefore more logical and representative of the actual situation to keep the grinding period constant, if no special separation of wastes is intended.

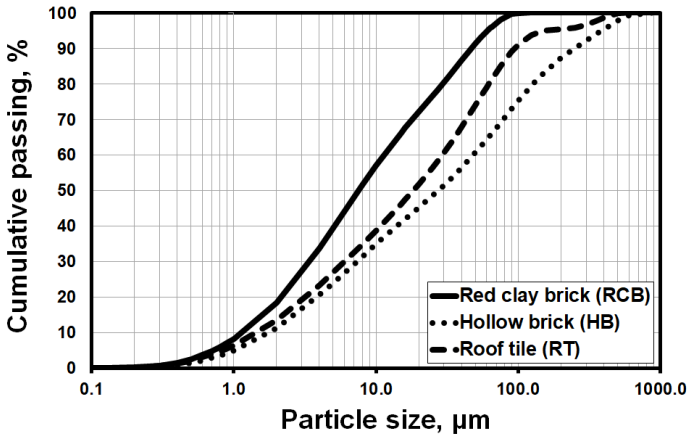

Fig. 2. Gradation curves of CDW-based precursors.

Table 1 Characteristic particle diameters of different CDW-based materials (units are in µm).

CDW-based material	Surface-weighted mean diameter ($D_{3,2}$)	Volume-weighted mean diameter ($D_{4,3}$)	D_{10}	D_{50}	D_{90}
Red clay brick (RCB)	2.9	16.4	1.2	7.6	46.9
Hollow brick (HB)	4.7	82.0	1.8	27.5	246.7
Roof tile (RT)	3.9	44.4	1.5	18.3	94.6

Table 2 Chemical compositions of CDW-based precursors as determined by XRF.

Chemical composition, %	CDW-based precursor		
	Red clay brick (RCB)	Hollow brick (HB)	Roof tile (RT)
Loss on ignition	2.18	1.99	2.11
SiO_2	53.4	61.6	54.0
Al_2O_3	20.5	17.3	15.9
Fe_2O_3	7.77	6.70	8.93
CaO	4.75	3.31	7.42
MgO	3.70	2.66	4.84
SO_3	1.16	0.38	0.68
Na_2O	1.53	1.61	1.41
K_2O	3.42	2.80	2.30

X-ray fluorescence (XRF) analysis was performed to determine the chemical composition of the CDW-based precursors and the results are shown in Table 2. The analysis showed that all precursors were rich in siliceous and aluminous oxides which are fundamentally important oxides for the alkali-activation. The total of siliceous and aluminous oxide compositions of

RCB (73.9%) and RT (69.9%) were found to be similar to each other while higher for HB (78.9%).

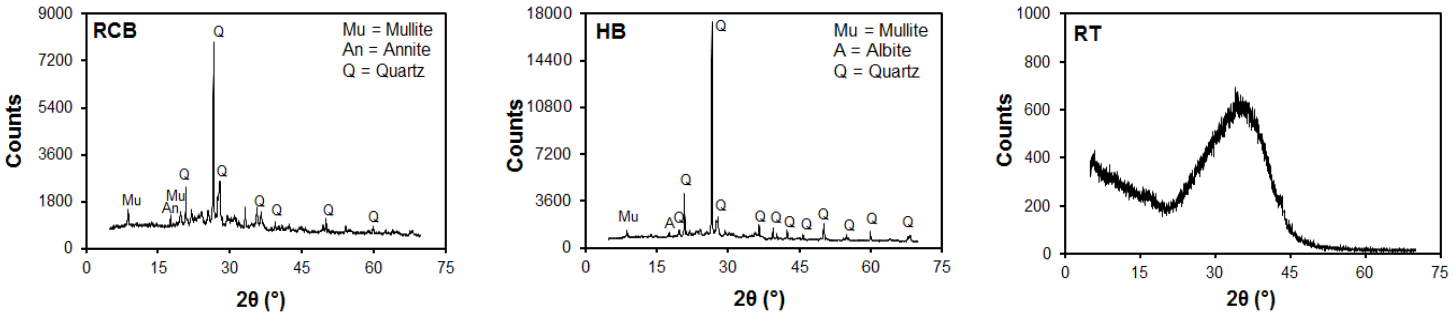

Fig. 3. XRD diffractograms of CDW-based precursors (Powder diffraction file [PDF] numbers: Mullite ($Al_{2.2}Si_{0.7}O_{4.8}$) PDF No: 96-900-1568, Albite ($NaAlSi_3O_8$) PDF No: 96-900-2201, Annite ($K_{0.94}Fe_{2.43}Al_{2.15}Si_{2.43}O_{12}$) PDF No: 96-900-2310, Quartz (SiO_2) PDF No: 96-101-1160.

X-ray diffraction (XRD) technique was also used to analyse the crystalline nature of the CDW-based precursors. As shown in Fig. 3, main crystalline peaks of RCB and HB were related to quartz (SiO_2, PDF No: 96-101-1160), mullite ($Al_{2.2}Si_{0.7}O_{4.8}$, PDF No: 96-900-1568), albite ($NaAlSi_3O_8$, PDF No: 96-900-2201) and annite ($K_{0.94}Fe_{2.43}Al_{2.15}Si_{2.43}O_{12}$, PDF No: 96-900-2310) while RT was amorphous with a broad hump centred between 2θ values of approximately 32º and 36º, although its production process involves very similar steps to that of RCB and HB. As it is well-known, clayey materials do not have pozzolanic activity and are crystalline/semi-crystalline in nature. However, when calcined at temperature ranges of 600-900 °C, they lose their combined water and their crystallographic structure collapses, leading to the formation of silica and alumina in an amorphous state or in a state characterized by disorder in the lattice structure. Under such circumstances, clay can exhibit pozzolanic activity since silica and alumina can react with calcium hydroxide [20]. However, when the calcination temperature exceeds 900 °C, reorganization of alumina and silica can take place, which leads to the formation of thermodynamically stable compounds such as mullite, tridimite etc. These compounds are also crystalline in nature and non-reactive with calcium hydroxide [20]. Today's so-called clayey building materials are rarely pozzolanic not only because they are calcined at higher temperatures but also they are composed of ingredients that contain no or low amounts

of clayey ingredients [20]. Based on these statements, it can be therefore stated that differences in the XRD diffractograms of CDW-based precursors can be largely related to the differences in the production processes, calcination temperature and raw materials used in these building materials [17,20]. Since the initial producer, production stages and the sources of CDW-based raw materials are not known, no further details related to the differences in the mineralogy of these materials can be provided.

CDW-based precursors were activated using a sodium hydroxide (NaOH) solution. The NaOH used for the preparation of the solution was in flake form and included a minimum 98% of sodium hydroxide, maximum 0.4% of sodium carbonate, 0.1% of sodium chloride and a maximum of 15 ppm iron.

2.2 Proportioning and mixing of alkali-activated binders

Preparation of alkali-activated binders essentially consisted of two steps: (i) preparation of the alkaline activator and (ii) the mixing of alkaline activator with the precursors. While preparing the alkaline activator, NaOH flakes were first dissolved in tap water at varying Na^+ concentrations of 7.36, 11.04 and 13.98% which corresponded to NaOH molarities of 10, 15 and 19M, respectively. After dissolving, the solutions were allowed to cool down in a laboratory environment set at room temperature. As mentioned previously, alkali-activated binders were produced by the binary combinations of different CDW-based precursors. All mixtures were produced with a constant water/binder ratio of 0.32 and incorporated a constant total amount of binder (1000 g). Depending on the mixture composition, each binary combination of CDW-based precursors (i.e. RCB-RT, RCB-HB and RT-HB) changed by 75-25%, 50-50% and 25-75% of the total weight of the binder. The mixture proportions of the alkali-activated binders are provided in Table 3 in more detail. No additional chemical admixtures were used in the mixtures to avoid any interactions that may occur with the alkaline solution.

Table 3 Mixture proportions of CDW-based alkali-activated binders.

Mixture ID.	Precursor, g			Alkaline solution				Alkaline activator/binder ratio
	RCB	HB	RT	Na, %	NaOH molarity, M	NaOH, g	Water, g	
75RCB-25RT	750	-	250	7.36	10	128.0	320	0.448
50RCB-50RT	500	-	500	11.04	15	192.0	320	0.512
25RCB-75RT	250	-	750	13.98	19	243.2	320	0.563
75RCB-25HB	750	250	-	7.36	10	128.0	320	0.448
50RCB-50HB	500	500	-	11.04	15	192.0	320	0.512
25RCB-75HB	250	750	-	13.98	19	243.2	320	0.563
75RT-25HB	-	250	750	7.36	10	128.0	320	0.448
50RT-50HB	-	500	500	11.04	15	192.0	320	0.512
25RT-75HB	-	750	250	13.98	19	243.2	320	0.563

At the mixing stage, the selected binary combinations of precursors were first loaded into a mortar mixer and mixed for 60 s. Then, the solution of the alkaline activator was slowly added to the mixer during the course of 30 s. After that, mixing was continued for 210 s at low speed. Finally, after a 15 s of waiting period during which the blade and cone of the mixer were cleaned, mixing was continued for 60 s at high speed to complete the mixing.

2.3 Specimen preparation, curing and testing

Current work included compressive strength testing and detailed microstructural assessment of alkali-activated binders for the performance characterization. For compressive strength tests, fresh mixtures were cast into cubic moulds with 50 mm dimensions and immediately after the completion of molding, specimens with their molds were placed into an oven and subjected to heat curing at the temperatures of 95, 105, 115 and 125°C for a period of 1, 2 and 3 days. Upon completion of curing, the cubic specimens were directly tested under uniaxial compressive loading applied at a rate of 0.9 kN/s. For a certain alkaline activator molarity, curing temperature/period and combination of CDW-based precursors, six specimens were tested and the obtained results were averaged for the determination of the compressive strength.

Microstructural characterization of the alkali-activated binders included the performance of X-ray diffraction (XRD) analyses and scanning electron microscopy observations coupled with energy-dispersive X-ray spectroscopy (SEM/EDX). XRD is a non-destructive method that is

able to analyse the crystalline structure of materials with the diffraction of X-rays. The diffraction profile identifies the crystalline phases and thereby the chemical composition of the material. In the experiments, XRD analyses were performed at a scan range of $5° \leq 2\theta \leq 80°$, with a 2θ step length of 0.033°, scanning step time of 30.48 s and for the wavelength $K\alpha 1$ of copper (λ = 1.5406 Â). Powder samples weighing approximately 20 mg were obtained from selected cubic alkali-activated binder specimens left from the compressive strength testing and used for the XRD analyses. Comparisons were then made between the XRD results of raw precursors and the alkali-activated binders. Similarly, samples with dimensions less than 1 cm were obtained from the selected specimens of compressive testing and used for SEM/EDX analyses. SEM micrographs were recorded and chemical formulations of the selected areas were further analysed by EDX.

3. Results and Discussion

3.1 Compressive strength

The average compressive strength results of the alkali-activated binders with different substitution rates of RCB-RT, RCB-HB and RT-HB are shown in Figs. 4-6, respectively with respect to the differences in curing temperature/periods and NaOH solution molar ratios.

According to the data presented in Figs. 4-6, the lowest compressive strength results were recorded at the curing temperature of 95 ºC for all proposed systems. However, despite the lower values, results well higher than 30 MPa were easily obtainable depending on the parameters of the alkali-activated binders.

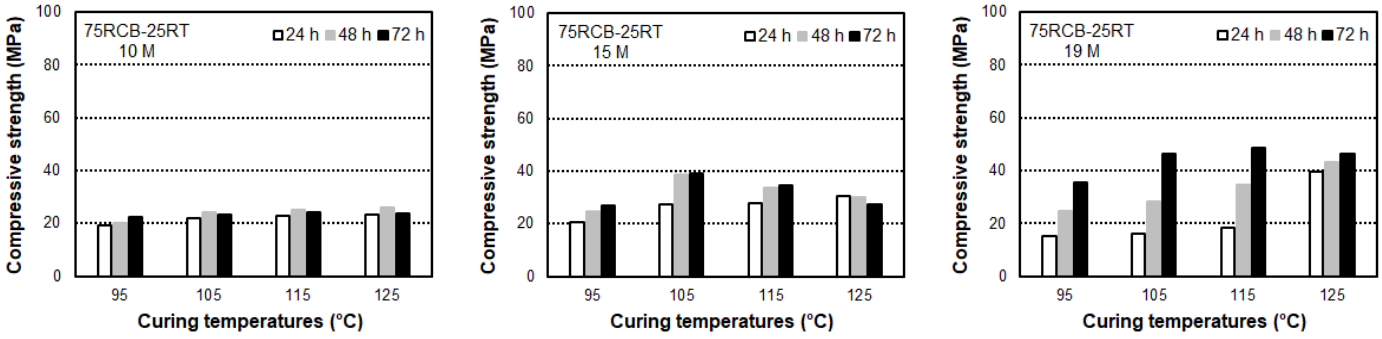

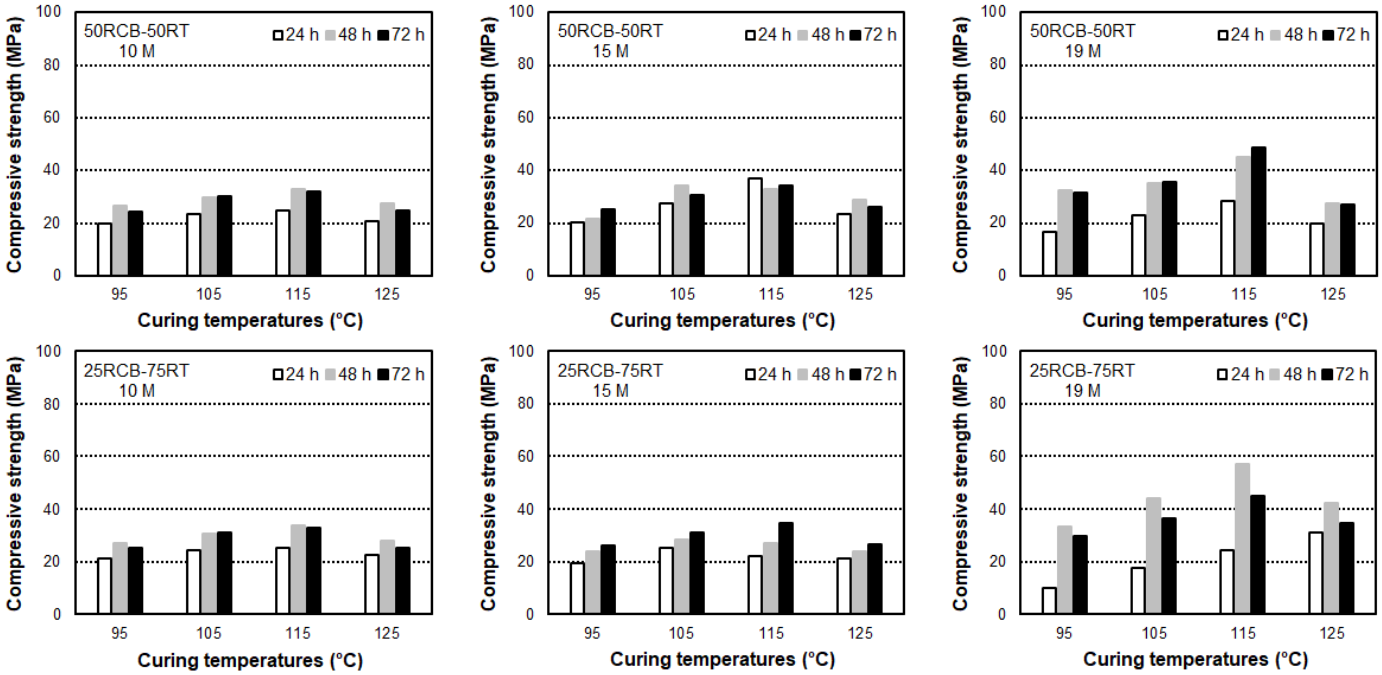

Fig. 4. Average compressive strength results of alkali-activated binders with different substitution rates of RCB and RT.

When the curing temperature was increased, the results mostly exhibited an incremental trend irrespective of the differences in precursors (Figs. 4-6). The effect of increased temperatures on the compressive strength of alkali-activated binders can be more understandable by looking at the processes involved in alkali activation process. On a general perspective, three main steps can be mentioned related to the processes of the formation of an alkali-activated (geopolymer) system. In the first step, continuous dissolution takes place from the surface of the aluminosilicate precursors to form tetrahedral units of SiO_4 and AlO_4 as a result of the breakage of Si – O – Si and Si – O – Al bonds in the presence of hydroxide ions. Secondly, the precursors and alkali polysilicates partially restructure and tetrahedral units of SiO_4 and AlO_4 are linked alternatingly to yield amorphous alkali-activated binders. Finally, the entire system re-precipitates leading to the settlement of an inorganic cross-linked 3-dimensional network [21]. At higher temperatures, initial dissolution of the aluminosilicate precursors gets faster due to increased activity of hydroxide ions of alkaline solution [22,23], which also accelerates the polycondensation reactions, hard structure formation and relatedly compressive strength results [23,24]. As the supersaturation point gets nearer, the process of

polycondensation takes the place of dissolution predominantly, which expels the water available in the solidified gels. At this stage, the dissolved phases very rapidly polymerize and reprecipitate, the rearrangement/polymerization of precursors take place and some of the alkali cations (Na^+) are bonded to the aluminosilicate gel network. It appears that at higher temperatures of curing, the processes mentioned above are completed earlier [23], which results in higher grades of compressive strength.

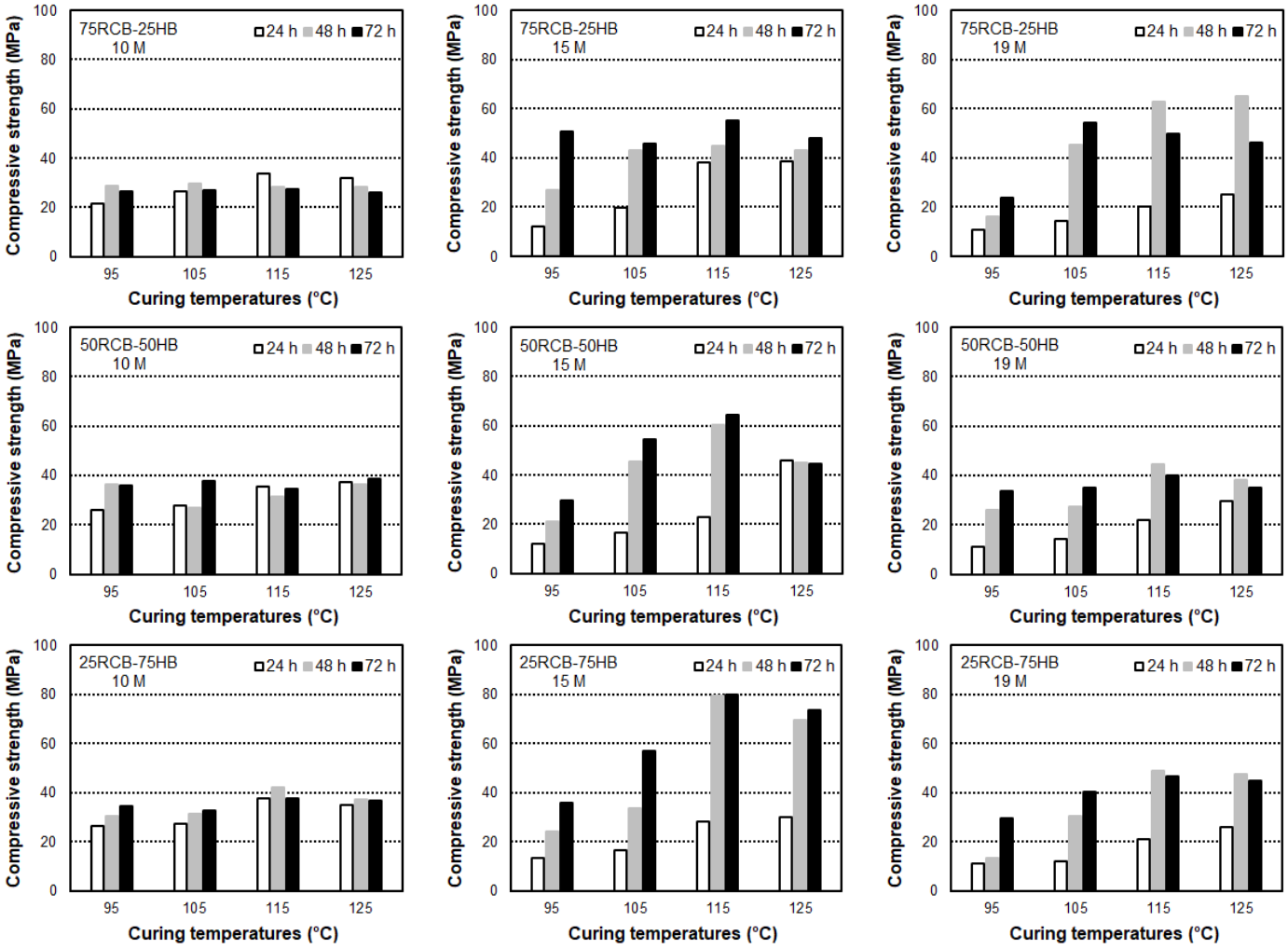

Fig. 5. Average compressive strength results of alkali-activated binders with different substitution rates of RCB and HB.

For most of the alkali-activated binder mixtures, continuous increments in the compressive strength results did not continue with the continuous increments in curing temperatures. At a certain curing temperature, the compressive strength results peaked and after exceeding this level of curing temperature, results either did not significantly change or decreased (Figs. 4-6).

This finding implies that temperature is a parameter which needs to be optimized to reach the highest level of improvement in the microstructures of alkali-activated binders. For alkali-activated binders with different substitution rates of RCB-RT, RCB-HB and RT-HB the level of curing temperature for the achievement of the highest compressive strength results was recorded to be mostly 115 ºC. Some of the alkali-activated binders, exhibited maximum compressive strength results at the curing temperature of 125 ºC as well (Figs. 4-6), however, in most of the cases, results either did not increase too much or decreased at this temperature level.

At highly elevated curing temperatures (e.g. 125 ºC herein), fast increments in the viscosity of alkali-activated binder structure can take place with the start of polycondensation and the capture and reaction of aluminosilicate species released after the precursors' dissolution. These phenomena occur rapidly and cause the alkali-activated binders to set promptly. The chance for clotting of the alkali-activated binder slurry increases with the rapid setting, which also increases the chance for undissolved aluminosilicate precursors to be covered. By this way, further dissolution of the precursors is prevented and the transformation from diffluent to a hard and more compact structure is limited. Beyond the optimum curing temperatures (mostly 115 °C in this study), elevated temperatures can also cause the contraction of alkali-activated binder gels due to excessive shrinkage/dehydration [24] and consequently cracking at microscale, all of which could be responsible for the stabilization or reduction of the compressive strength. Furthermore, the stabilization or reduction of the compressive strength can also be associated with the possible effects of highly elevated temperatures on the quality of alkali-activation products. When samples are cured at optimum curing temperatures that are not excessively high for a certain mixture proportion, an alkali-activated binder structure that is low-porosity and high-toughness forms since the reaction products find enough time to slowly fill the pores. On the other hand, when the curing temperature is higher than the optimum curing temperature,

279 although the reactions take place very rapidly, a less ordered and more porous structure with
280 lower-quality reaction products forms which may lower the compressive strength [23]. It can
281 be stated here that although the negative and positive effects of high temperature curing are
282 expected to be present for all the curing temperatures utilized in the study, for highly elevated
283 temperatures (125 °C), negative effects seem to outweigh the positive effects and lower the
284 compressive strength results.

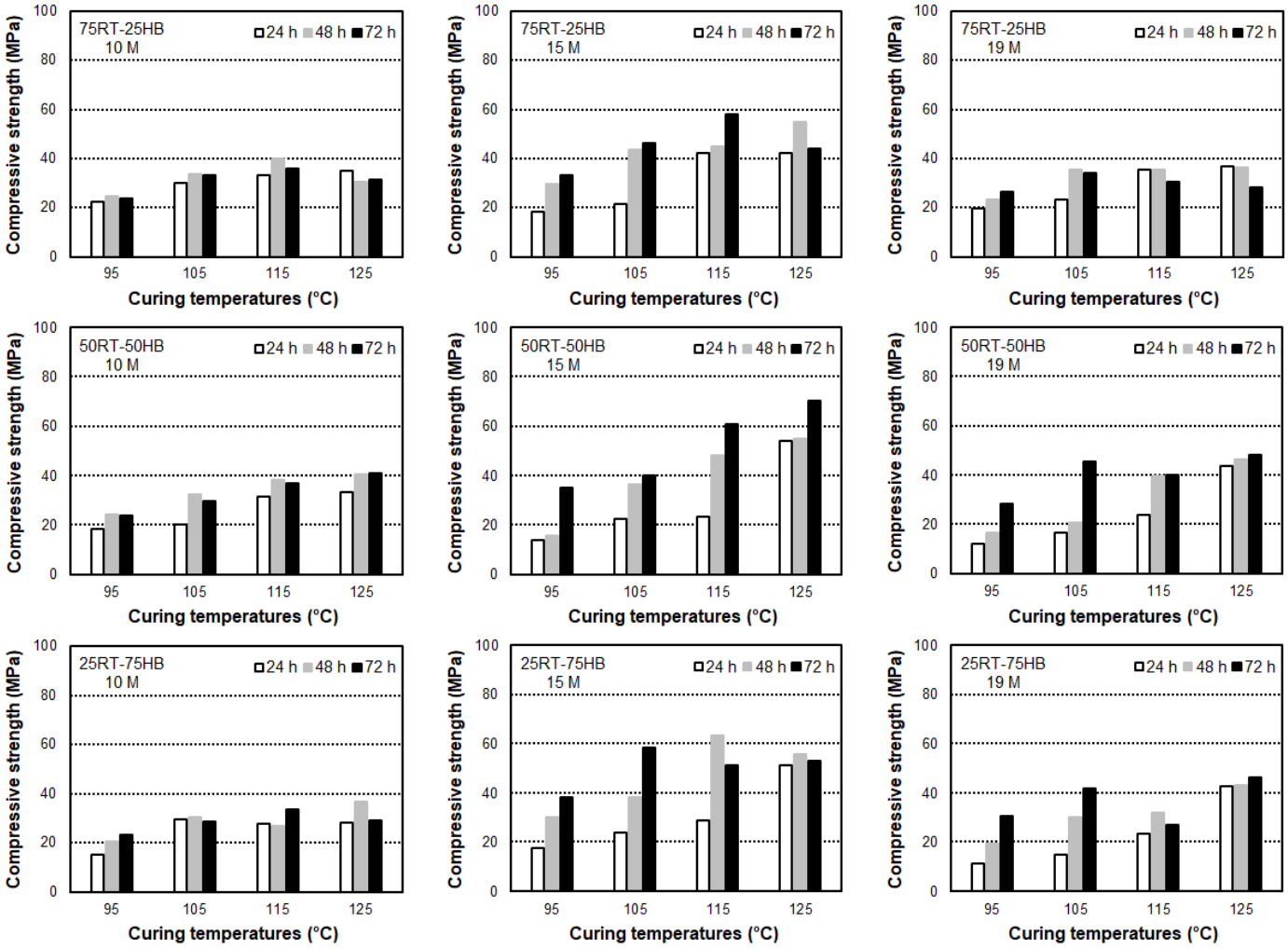

285 **Fig. 6.** Average compressive strength results of alkali-activated binders with different
286 substitution rates of RT and HB.
287

288 When the curing period was extended, compressive strength results of the alkali-activated
289 binders mostly increased. The increments in the results were clearer from 24 h to 48 h. When
290 the curing period was extended from 48 h to 72 h, there were quite a number of cases where
291 either slight changes or reductions in the compressive strength results of alkali-activated binders

were noted (Figs. 4-6). Moreover, for the majority of specimens tested, 24 h of heat curing was adequate to obtain the large share of the ultimate compressive strength that will be reached after 72 h of heat curing. This therefore implied that curing at elevated temperatures for longer periods is not always an effective way to improve the compressive strength of alkali-activated binders [25]. The positive outcomes of curing for longer periods are related to the beneficial effects of curing at higher temperatures on the previously-noted steps of alkali activation process. Possible reasons for the slight changes or reductions noted in the compressive strength results of certain specimens with the prolonged periods of heat curing can be related to the breakdown of the gelular structure of alkali-activated binder, occurrence of gel contraction, dehydration and excessive shrinkage without transforming into a more semi-crystalline form, the changes in the amorphous phase of gel formation as the crystalline part of the alkali-activated binder is not affected by the longer periods of exposure to heat curing and the inadequate availability of certain amount of water to eliminate cracking and maintain structural integrity [26-28].

When the molarity of NaOH solution was increased, compressive strength results generally increased, although there were also clear deviations from this trend depending on the curing temperature/period and the selected precursor type/substitution ratios, especially when the molarity of the alkaline solution was increased from 15M to 19M (Fig. 4). In most of the models proposed for the alkali activation, consecutive events of dissolution, orientation and reprecipitation of precursors and alkaline activators are reported [29]. Among these events, dissolution is regarded to be the most critical since it plays certain roles in relation to the liberation of substances to be used in the formation of SiO_4 and AlO_4 tetrahedral units and in activating the surface bonding reaction (polymerization). The latter strongly contributes to the final strength of the alkali-activated binder structure [30,31]. In line with these statements, the higher compressive strengths of alkali-activated binders produced with higher molarities of

NaOH solution can be attributed to the better ability of the highly concentrated NaOH solution to dissolve the CDW-based precursors and form a polymerized network having strengthened link with the dissolved particles of the precursors [32]. On the other hand, reductions noted in the compressive strength results with the increased NaOH solution molarities depending on the other mixture parameters were attributed to the coagulation of silica [33,34] and faster setting which does not allow for a homogenous mixing resulting in a poor and incipient polymerization [35].

Activators are usually the most expensive components of alkali-activated binders or geopolymers [12] and their optimization is therefore desirable, taking the cost and environmental impact considerations into account. It is important to state that although increased compressive strength results were recorded from alkali-activated binders with NaOH solutions having higher molarities on a general perspective, reasonable compressive strength results which were in the range of 25-35 MPa were easily obtainable from the proposed alkali-activated binders even at NaOH molarity of 10M, depending on the combinations of precursors (Figs. 4-6).

Despite the certain differences in the physical properties (particle size and diameter [see Fig. 2 and Table 1]) and chemical compositions (see Table 2) of RCB and RT, as detailed in Section 2.1, the utilization of these CDW-based precursors at different substitution rates did not create distinctive differences in the compressive strength results. As can be seen from Fig. 4, for each binary combination of RCB and RT, the compressive strength results are close when other mixture/production parameters are kept the same. This suggests that RCB and RT compensated for each other's drawbacks as precursors and more or less acted as a single precursor.

At similar substitution ratios, the average compressive strength results of RCB-HB-based alkali-activated binders were found to be comparably higher than those of RCB-RT-based alkali-activated binders, especially when the curing periods were extended, which showed that

342 the utilization of HB instead of RT promoted the achievement of higher strength grades.
343 Depending on the other mixture parameters, it was possible to reach an average compressive
344 strength value of 80 MPa for RCB-HB-based alkali-activated binders (e.g. 25RCB-75HB
345 specimens produced with 15M of NaOH solution and cured at 115 ºC for 48h and 72h) (Fig.
346 5). Alkali activation is affected to a great extent by the chemical composition, solubility, particle
347 size distribution/fineness and the degree of amorphousness of precursors. The alkali activation
348 capability of the aluminosilicate precursors is usually perceived to be more pronounced when
349 highly amorphous structure, high amounts of siliceous/aluminous oxides and smaller grain size
350 are present. In addition, it has been reported that significantly higher compressive strength
351 results could be obtained from alkali-activated binders when the particle fractions of precursors
352 are kept under 150 μm and the D_{50} value is less than 15 μm [13]. As can be seen in Table 1,
353 Fig. 2 and Fig. 3, among all CDW-based precursors used in this work, HB had D_{50} value of 27.5
354 μm, which was the coarsest in terms of the grain size and exhibited more distinctive crystalline
355 peaks in the XRD analysis, all of which contradicting with the abovementioned parameters that
356 nourish a better alkali activation capability in general. On the other hand, HB possessed a higher
357 total amount of siliceous/aluminous oxides (78.9%) compared to RCB (73.9%) and RT
358 (69.9%). The relationship between the compressive strength results, physical properties and
359 chemical composition of precursors, therefore showed that despite the importance of other
360 properties of the precursors, their chemical composition (i.e. aluminosiliceous material
361 composition) has a more decisive influence on the compressive strength results. This result was
362 also found to be in concordance with the study of De Silva et al. [22] who stated that even the
363 minor changes in the available Si and Al concentrations during alkali activation can drastically
364 affect the properties of the ultimate alkali-activated binder.
365 As the chemical compositions of different CDW-based precursors are quite similar to each
366 other (Table 2), one might still consider if this much of a small difference can lead to such

differences in the compressive strength results of the alkali-activated binders. In this regard, the study of Van Jaarsveld et al. [36] also concluded similar findings for fly ash-based geopolymers. They reported that two types of fly ash which were acquired from the same source and had nearly identical average particle sizes with only slight differences in their CaO contents, showed significantly different setting behaviours. This difference was associated with the greater tendency of one of the fly ashes to aggregate more within the aqueous media due to the differences in the surface charge of particles. It was concluded in this sense that zeta-potential of fly ash can be decisive on the observed differences in the setting and dissolution rate of fly ash [36]. This behaviour mentioned in [36] is also likely to cause the differences noted in the compressive strength results of alkali-activated binders with CDW-based precursors having rather similar chemical compositions.

With the increased substitution rates of HB, a general incremental trend in the compressive strength results of RT-HB-based alkali-activated binders was observed, especially for specimens cured for longer periods. In addition, the compressive strength results of RT-HB-based alkali-activated binders (Fig. 6) were higher than RCB-RT-based alkali-activated binders (Fig. 4), which again showed the positive effects of the utilization/increased amounts of HB in the alkali-activated binder production. When the plots shown in Figs. 5 and 6 are compared, it can be seen that the compressive strength results of RCB-HB-based alkali-activated binders are slightly higher than RT-HB-based alkali-activated binders, which suggested that RCB worked better with HB and favoured the strength evolution. The better synergy of RCB with HB compared to RT can be explained by the smaller particle diameter/gradation (see Table 1 and Fig. 2) and the higher total amount of siliceous/aluminous oxides (Table 2) in RCB compared to RT. The comparatively higher amount of CaO (7.42%) available in the composition of RT with respect to other precursors having maximum CaO content of 4.75% may have also contributed to the slightly lower compressive strength results in the RT-HB-based geopolymers.

As the Ca^{+2} species dissolve from aluminosilicate material in high alkaline medium and react with OH^- ions in the system, a decrease in strength results can be observed as a result of lowering the pH of the system and precipitation as $Ca(OH)_2$ [13,37]. CaO can also react with SiO_2 phases and result in calcium-silicate-hydrate (CSH) gels similar to the case observed in Portland cement-based systems. However, the amount of CaO, even in RT, is relatively low for the precursors used herein to assure stable CSH gel formation therefore, calcium-based gel formation was not observed as also explained in the following sections.

3.2 Microstructural characterization

3.2.1 X-ray diffraction (XRD)

In Fig. 7, the selected XRD diffractograms of alkali-activated binders produced with different substitution rates of CDW-based precursors are shown. For further discussions, the mixture parameters that generally yielded optimum compressive strength results for the alkali-activated binders are chosen. Therefore, the XRD diffractograms belonging to alkali-activated binders activated with 15M NaOH solution and cured at 115 ºC for 48 hours are the ones incorporated in Fig. 7. It needs to be stated here that although the intensity of peaks and the ultimate alkali activation products changed with regard to the rest of the mixture design parameters, these changes were not dramatic, suggesting that the results presented in Fig. 7 are representative of a general behaviour.

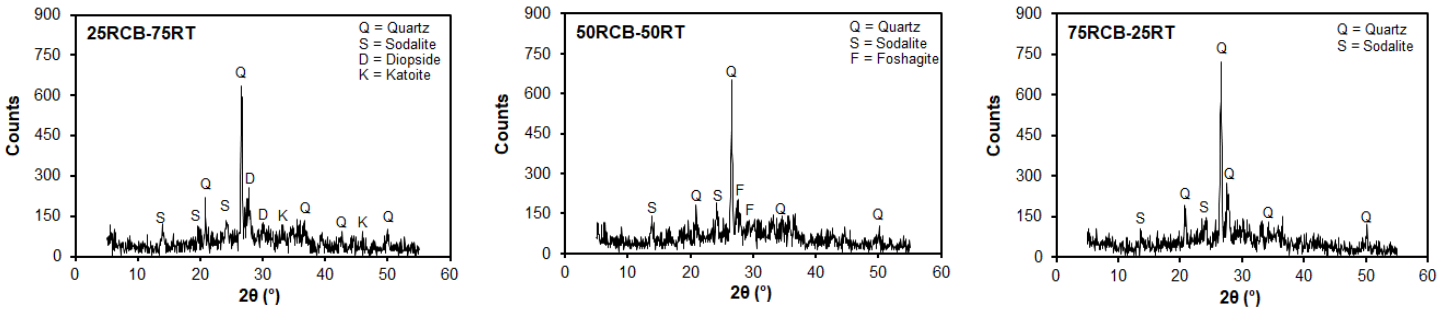

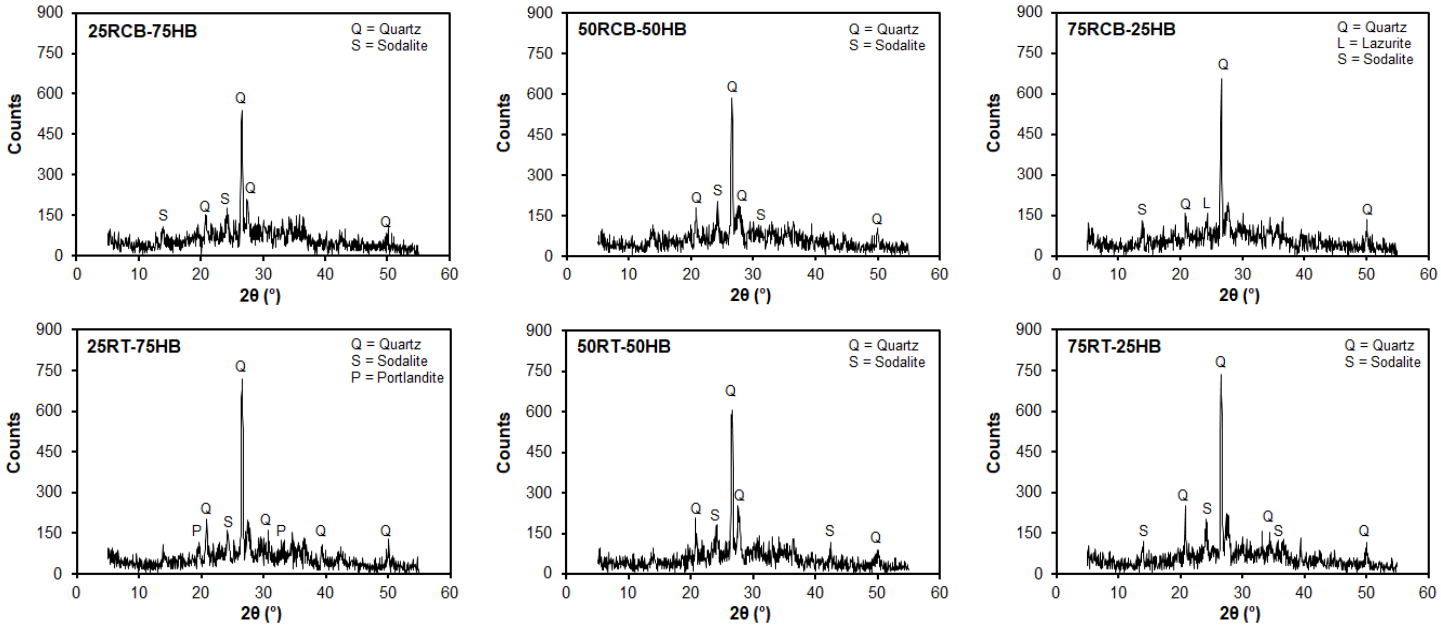

Fig. 7. XRD diffractograms of alkali-activated binders having different substitution rates of CDW-based precursors, activated with 15M NaOH solution and cured at 115 ºC for 48 hours. [Quartz (SiO_2) PDF No: 96-101-1160, Sodalite ($Na_4Al_3Si_3O_{12}Cl$) PDF No: 96-900-3326, Diopside ($CaMg_{0.7}Si_{1.7}O_6$) PDF No: 96-900-5280, Katoite ($Ca_3Al_2Si_3O_{12}H_{12}$) PDF No: 96-900-2709, Foshagite ($Ca_4Si_3O_{11}H_2$) PDF No: 96-901-1044, Lazurite ($Na_{3.48}Ca_{0.6}Al_{2.91}Si_{3.09}O_{11.52}S$) PDF No: 96-901-1357, Portlandite ($Ca(OH)_2$) PDF No: 96-900-6836]

As can be seen from the XRD diffractograms of the raw precursors (Fig. 3), RCB and HB are crystalline in nature while RT is amorphous. Alkali-activated binders (geopolymers) are amorphous to X-rays, although there is also clear evidence in the literature that final alkali activation products can show structure ranging from amorphous to near-crystalline [26]. In the case of current research, for all of the studied mixtures, the XRD diffractograms of the alkali-activated binders exhibited clear crystalline peaks. However, evidently, the intensity of peaks of the raw precursors (Fig. 3) either significantly decreased or changed into crystals with different nature (Fig. 7). Decrements and/or changes in the XRD patterns of alkali-activated binders were anticipated and suggestive of the occurrence of alkali-activation, since these minerals of precursors are used in the dissolution/reorganization steps of alkali activation. Studies available in the literature also found clear peaks visible to X-rays after XRD analyses [19,38]. Those studies attributed the availability of such crystalline phases in alkali-activated binders to the unreacted feedstock of crystal phases of the precursors and/or formation of

zeolitic structures, overlapping the amorphous baseline, particularly when highly concentrated NaOH is used as the activator [19,38].

It was reported in [39] that the formation of different zeolitic reaction products is affected by the molarity of the NaOH solution and when the molarities higher than 5M are targeted (similar to the cases here), cancrinite group of minerals (e.g. herschelite, hydroxysodalite or hydroxycancrinite) are usually generated. These minerals, in terms of their crystal structure, show similarities to the zeolitic minerals. Similar findings are also reported in [40,41] where it was concluded that sodium aluminosilicate (N-A-S-H) gel is the main reaction product for fly ash-based alkali-activated materials. N-A-S-H is also the main reaction product of the alkali-activated binders of the current study, as will be detailed in the following section. Due to their medium/long-range disorder, N-A-S-H gels were reported to be X-ray amorphous, however, the gels were also found to show zeolite-like three-dimensional structure at nano-scale [40]. In accordance with [42,43], this confirms that N-A-S-H gel is a zeolite precursor with a thermodynamic tendency and has a high likelihood to crystallize into a zeolite, which may explain the evident crystalline peaks observed in this study after alkali activation process.

As can be seen from Fig. 7, after alkali activation, irrespective of the different substitution rates of precursors, peaks of mullite, annite and albite in the precursors disappeared entirely and crystalline peaks related to quartz (SiO_2, PDF No: 96-101-1160), sodalite ($Na_4Al_3Si_3O_{12}Cl$, PDF No: 96-900-3326), diopside ($CaMg_{0.7}Si_{1.7}O_6$, PDF No: 96-900-5280), katoite ($Ca_3Al_2Si_3O_{12}H_{12}$, PDF No: 96-900-2709) foshagite ($Ca_4Si_3O_{11}H_2$, PDF No: 96-901-1044), lazurite ($Na_{3.48}Ca_{0.6}Al_{2.91}Si_{3.09}O_{11.52}S$, PDF No: 96-901-1357 and portlandite ($Ca(OH)_2$, PDF No: 96-900-6836) were visible.

Among alkali activation products which were visible under X-rays, only sodalite constitutes an ion (chloride [Cl^-]) which was not available in the compositions of CDW-based precursors (Table 2, Fig. 3). Available Cl^- ions in sodalite mineral are most likely to be originated from the

NaOH solution which incorporates certain amount of sodium chloride, as noted in Section 2.1. As seen from Fig. 7, peaks of quartz and sodalite were both clearer and higher in intensity for all alkali-activated binders in addition to the less intensified peaks of lazurite, diopside, katoite, foshagite and portlandite. Peaks related to quartz and zeolite type minerals such as sodalite and lazurite were noted in alkali-activated binders produced with Al-rich precursors [39,44]. Peaks related to lazurite, diopside, katoite, foshagite and portlandite were associated with the reactions between precursors and NaOH solution involving the participation of CaO and MgO, depending on the resultant mineral type. As discussed in the literature, it is assumed that the calcium species dissolved from aluminosilicate based precursors will precipitate as portlandite at the initial dissolution stage in an alkaline environment, and will participate in the formation of C-S-H gel at later stages [10,45]. However, these peaks were not of high intensity, therefore minerals related to these peaks did not play a decisive role in changing the overall nature of ultimate alkali activation reaction products, as discussed in the following section. Calcination of clayey materials at temperatures higher than 950 ºC leads to the formation of mullite crystals, which are stated to be non-reactive in alkaline activation [46]. In this study, however, mullite crystals available in some of the precursors disappeared after alkali activation, which was an outcome concordant with several literature studies [42,47] that stated it was possible to change the mullite crystals under strongly alkaline environments.

When compared to each other, it was not easy to clearly comment on the relationship between the values of compressive strength and the XRD diffractograms of the alkali-activated binders produced with different binary substitutions of CDW-based precursors. The intensities and types of crystalline peaks were similar to each other. However, it can be stated based on Fig. 7 that when the amount of HB was increased in the alkali-activated binder mixtures (especially for RCB-HB binary combination), the intensity of the main quartz peaks started to

be less pronounced, suggesting better alkali activation process. This fact can be related to the higher compressive strength results of corresponding specimens as discussed formerly.

3.2.2 Scanning electron microscopy (SEM/EDX)

In this section, the products that were formed after the alkali activation is detailed considering the SEM micrographs, supported by EDX analyses, performed on the selected regions. Similar to the XRD results, the analyses are focused on alkali-activated binders having different substitution rates of CDW-based precursors, activated with 15M NaOH solution and cured at 115 ºC for 48 hours. To be more concise, Figs 8-10 show the SEM/EDX analyses on alkali-activated binders with the precursor combinations of 25RCB-75RT, 25RCB-75HB, 25RT-75HB mixtures that showed different levels of compressive strength for the selected molarity and curing conditions, respectively.

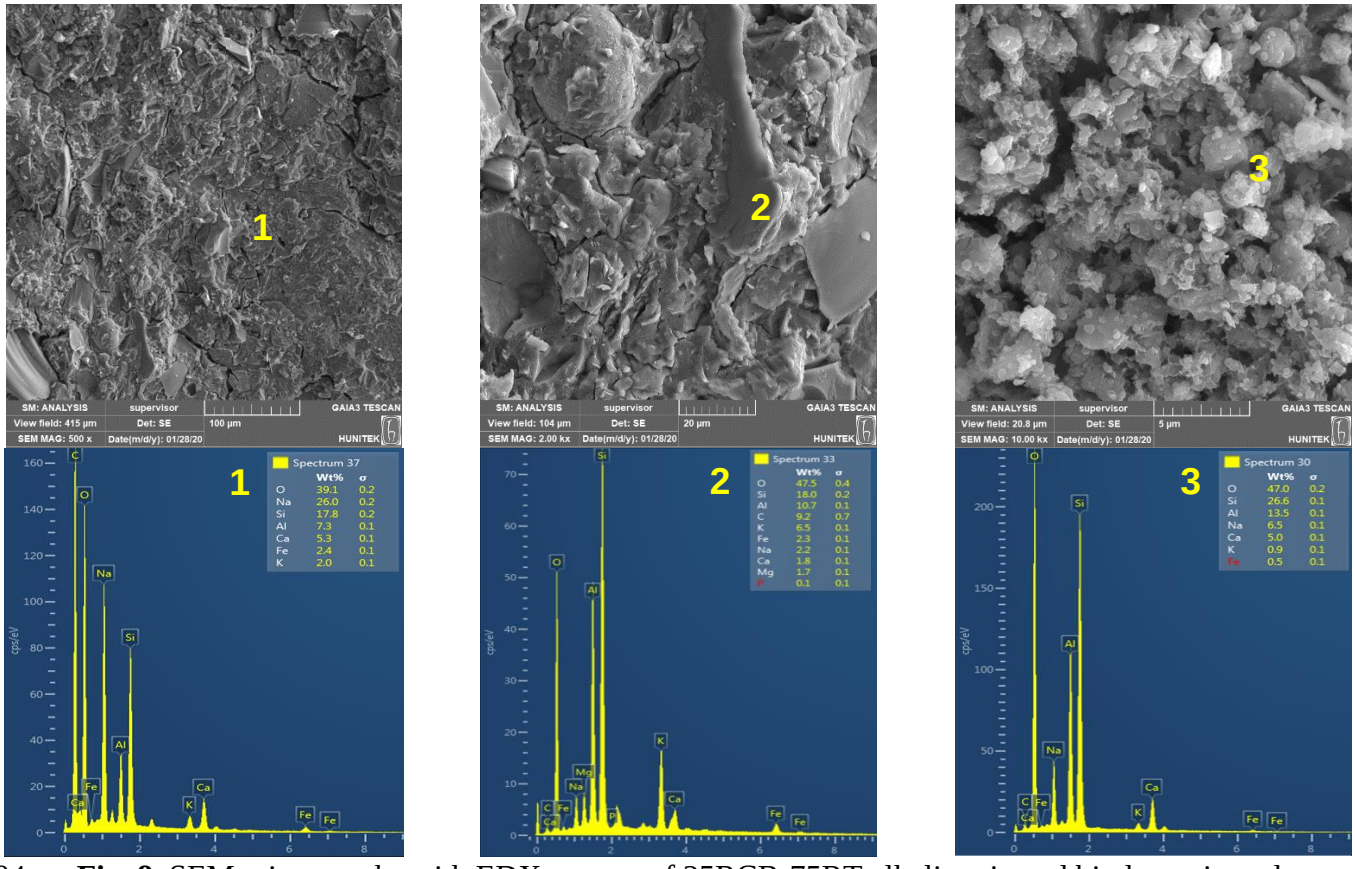

Fig. 8. SEM micrographs with EDX spectra of 25RCB-75RT alkali-activated binder activated with 15M NaOH solution and cured at 115 ºC for 48 hours.

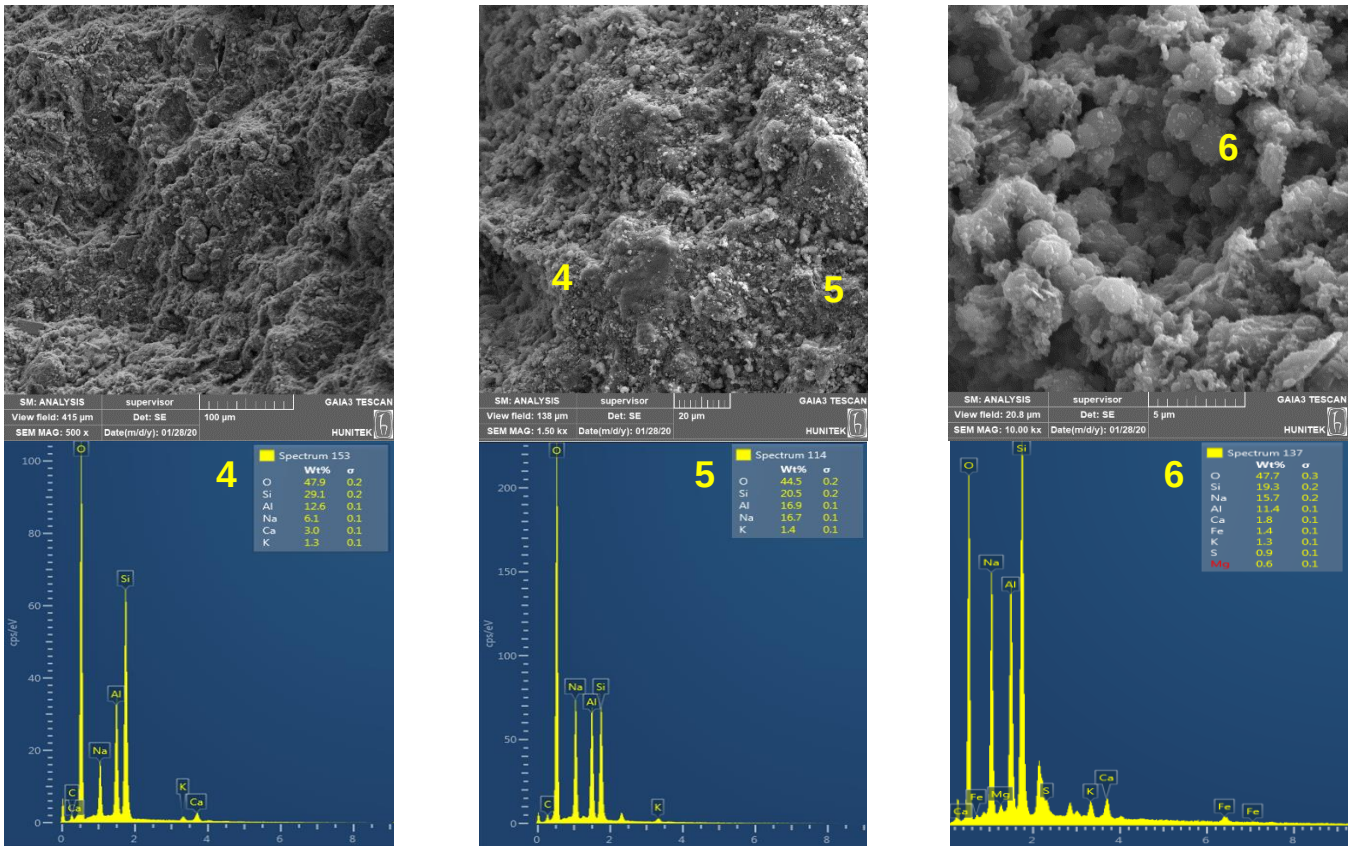

Fig. 9 SEM micrographs with EDX spectra of 25RCB-75HB alkali-activated binder activated with 15M NaOH solution and cured at 115 ºC for 48 hours.

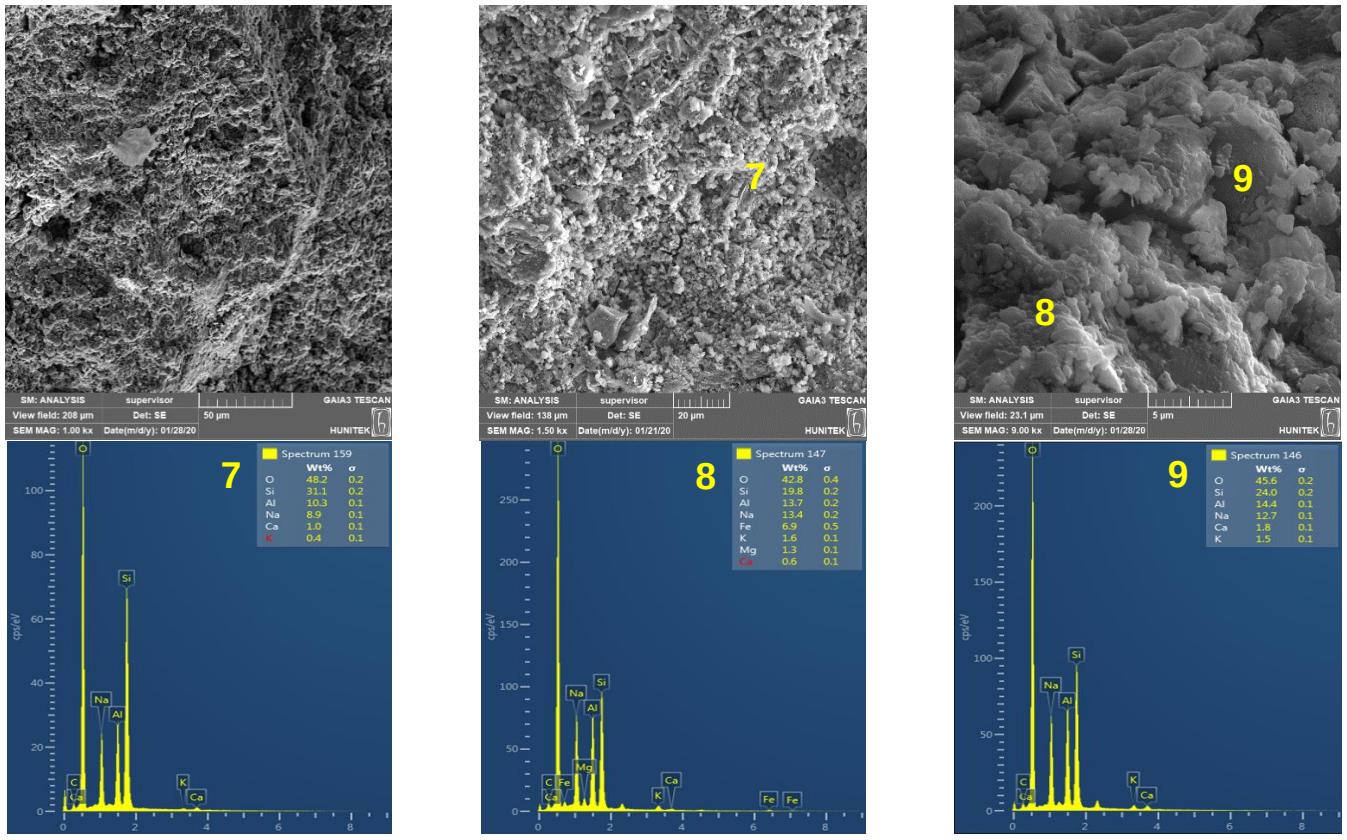

Fig. 10. SEM micrographs with EDX spectra of 25RT-75HB alkali-activated binder activated with 15M NaOH solution and cured at 115 ºC for 48 hours.

When compared to the SEM photos of precursors shown in Fig. 1, clearly, significant improvements and densifications took place in the microstructures of the mixtures after alkali activation, irrespective of the way the precursors were combined. Furthermore, there were differences noted in the microstructures of different alkali-activated binders, although not that substantial. As can be seen in Fig. 8, there are certain microcracks, irregularities in the distribution of the ultimate products and also undissolved raw materials available in the microstructure of the 25RCB-75RT-based alkali-activated binders. However, the microstructures of the 25RCB-75HB and 25RT-75HB-based alkali-activated binders did not show microcracking presence .Those alkali-activated binders were more compact, with more uniformly distributed products and with less undissolved raw materials (especially those with 25RCB-75HB [Fig. 9]). These findings for different alkali-activated binders are in line with the compressive strength results discussed previously.

For all the samples, clear peaks of Na, Al and Si with different intensities were observed in the EDX spectra, in addition to crystal-like structures observed in the SEM micrographs. These findings therefore suggest that the main reaction products of the alkali-activated binders produced here are N-A-S-H gels, which are combined with zeolitic polytypes (e.g. sodalite, lazurite) having a structure ranging from amorphous to polycrystalline. It must be also noted that there are slightly visible Ca peaks in the 25RCB-75RT-based alkali-activated binders, which were also evidenced in the XRD results in the form of CaO bearing minerals such diopside and katoite and was found attributable to the higher CaO content of RT.

4. Conclusions

This study showed that precursors obtained from CDW-based masonry units can be used together in the production of alkali-activated binders. It is notable that this can be achieved by a simple combination of these units at different proportions rather than using them singly, which requires selective demolishing practises/individual separation and can be time-

consuming/energy-inefficient. Additionally, the following conclusions were drawn from the current research:

- The compressive strength of alkali-activated binders from precursors of CDW-based masonry tends to increase with the increments in curing temperature/period, molarity of NaOH used as the alkaline activator and the increased amounts of HB in precursor combinations. The highest compressive strength results were generally reached at curing temperature/period and NaOH solution molarity of 115°C/48 hours and 15M. Using these mixture design parameters, compressive strength values as high as 80 MPa could be obtained. Depending on different design parameters, compressive strength results ranging from 25 to 30 MPa are easily obtained even after 24 h of curing at 95 °C (which were the lowest curing temperature and shortest curing period used herein).
- The compressive strength results were largely concordant with the microstructural analyses. For all the alkali-activated binders, the main alkali activation products were N-A-S-H gels containing different zeolitic polytypes (e.g. sodalite, lazurite), which had a structure ranging from amorphous to polycrystalline nature.

Acknowledgements

The authors gratefully acknowledge the financial assistance of the Scientific and Technical Research Council (TUBITAK) of Turkey and British Council provided under projects: 117M447 and 218M102.

References

[1] Monteiro PJM, Miller SA, Horvath A. Towards sustainable concrete. Nat Mater 2017;16:698–9.

[2] Chen C, Habert G, Bouzidi Y, Jullien A. Environmental impact of cement production: detail of the different processes and cement plant variability evaluation. J Clean Prod 2010;18:478–85.

[3] Sahmaran M, Anil O, Lachemi M, Yildirim G, Ashour AF, Acar F. Effect of corrosion on shear behavior of reinforced engineered cementitious composite beams. ACI Struct J 2015;112:771–82.

[4] Alyousif A, Anil O, Sahmaran M, Lachemi M, Yildirim G, Ashour AF. Comparison of shear behaviour of engineered cementitious composite and normal concrete beams with different shear span lengths. Mag Concr Res 2016;68:217–28.

[5] Alyousif A, Lachemi M, Yildirim G, Aras GH, Sahmaran M. Influence of cyclic frost deterioration on water sorptivity of microcracked cementitious composites. J Mater Civ Eng 2015;28:04015159.

[6] Yildirim G, Sahmaran M, Al-Emam MKM, Hameed RKH, Al-Najjar Y, Lachemi M. Effects of compressive strength, autogenous shrinkage, and testing methods on bond behavior of high-early-strength engineered cementitious composites. ACI Mater J 2015;112:409–18.

[7] Sahmaran M, Al-Emam M, Yildirim G, Simsek YE, Erdem TK, Lachemi M. High-early-strength ductile cementitious composites with characteristics of low early-age shrinkage for repair of infrastructures. Mater Struct Constr 2015;48:1389–403.

[8] Wu H, Zuo J, Yuan H, Zillante G, Wang J. A review of performance assessment methods for construction and demolition waste management. Resour Conserv Recycl 2019;150:104407.

[9] Zheng L, Wu H, Zhang H, Duan H, Wang J, Jiang W, et al. Characterizing the generation and flows of construction and demolition waste in China. Constr Build Mater 2017;136:405–13.

574 [10] Provis JL, Van Deventer JSJ (Eds.). Alkali Activated Materials, State-of-the-Art Report,
575 RILEM TC 224-AAM. Springer/RILEM, Dordrecht, 2014.

576 [11] Provis JL. Alkali-activated materials. Cem Concr Res 2018;114:40–8.

577 [12] Shi C, Qu B, Provis JL. Recent progress in low-carbon binders. Cem Concr Res
578 2019;122:227–50.

579 [13] Komnitsas K, Zaharaki D, Vlachou A, Bartzas G, Galetakis M. Effect of synthesis
580 parameters on the quality of construction and demolition wastes (CDW) geopolymers. Adv
581 Powder Technol 2015;26:368–76.

582 [14] Lampris C, Lupo R, Cheeseman CR. Geopolymerisation of silt generated from
583 construction and demolition waste washing plants. Waste Manag 2009;29:368–73.

584 [15] Ahmari S, Ren X, Toufigh V, Zhang L. Production of geopolymeric binder from blended
585 waste concrete powder and fly ash. Constr Build Mater 2012;35:718–29.

586 [16] Vásquez A, Cárdenas V, Robayo RA, de Gutiérrez RM. Geopolymer based on concrete
587 demolition waste. Adv Powder Technol 2016;27:1173–9.

588 [17] Reig L, Tashima MM, Borrachero M V., Monzó J, Cheeseman CR, Payá J. Properties and
589 microstructure of alkali-activated red clay brick waste. Constr Build Mater 2013;43:98–106.

590 [18] Reig L, Tashima MM, Soriano L, Borrachero M V., Monzó J, Payá J. Alkaline activation
591 of ceramic waste materials. Waste and Biomass Valorization 2013;4:729–36.

592 [19] Sun Z, Cui H, An H, Tao D, Xu Y, Zhai J, et al. Synthesis and thermal behavior of
593 geopolymer-type material from waste ceramic. Constr Build Mater 2013;49:281–7.

594 [20] Baronio G, Binda L. Study of the pozzolanicity of some bricks and clays. Constr Build
595 Mater, 1997:11:41-46.

[21] Duxson P, Fernández-Jiménez A, Provis JL, Lukey GC, Palomo A, Van Deventer JSJ. Geopolymer technology: The current state of the art. J Mater Sci 2007;42:2917–33.

[22] De Silva P, Sagoe-Crenstil K, Sirivivatnanon V. Kinetics of geopolymerization: Role of Al_2O_3 and SiO_2. Cem Concr Res 2007;37:512–18.

[23] P. Rovnaník. Effect of curing temperature on the development of hard structure of metakaolin-based geopolymer. Constr Build Mater 2010;24:1176–83.

[24] Mo BH, Zhu H, Cui XM, He Y, Gong SY. Effect of curing temperature on geopolymerization of metakaolin-based geopolymers. Appl Clay Sci 2014;99:144–8.

[25] Memon FA, Nuruddin MF, Demie S, Shafiq N. Effect of curing conditions on strength of fly ash-based self-compacting geopolymer concrete. Int J Civ Environ Eng 2011;3:183–86.

[26] Van Jaarsveld JGS, Van Deventer JSJ, Lukey GC. The effect of composition and temperature on the properties offly ash- and kaolinite-based geopolymers 2002;89:63–73.

[27] Van Jaarsveld JGS, Van Deventer JSJ, Lorenzen L. Factors affecting the immobilization of metals in geopolymerized flyash. Metall Mater Trans B Process Metall Mater Process Sci 1998;29:283–91.

[28] Komnitsas K, Zaharaki D. Geopolymerisation: A review and prospects for the minerals industry. Miner Eng 2007;20:1261–77

[29] Xu H, Van Deventer JSJ. The geopolymerisation of alumino-silicate minerals. Int J Miner Process 2000;59:247–66.

[30] Phair JW, Van Deventer JSJ, Smith JD. Mechanism of polysialation in the incorporation of zirconia into fly ash-based geopolymers. Ind Eng Chem Res 2000;39:2925–34.

[31] Wu HC, Sun P. New building materials from fly ash-based lightweight inorganic polymer. Constr Build Mater 2007;21:211–17.

[32] Wang H, Li H, Yan F. Synthesis and mechanical properties of metakaolinite-based geopolymer. Colloids Surfaces A Physicochem Eng Asp 2005;268:1–6.

[33] Atis CD, Gorur EB, Karahan O, Bilim C, Ilkentapar S, Luga E. Very high strength (120 MPa) class F fly ash geopolymer mortar activated at different NaOH amount, heat curing temperature and heat curing duration. Constr Build Mater 2015;96:673–78.

[34] Rattanasak U, Chindaprasirt P. Influence of NaOH solution on the synthesis of fly ash geopolymer. Miner Eng 2009;22:1073–78.

[35] Palomo A, Grutzeck MW, Blanco MT. Alkali-activated fly ashes: A cement for the future. Cem Concr Res 1999;29:1323–29.

[36] Van Jaarsveld JGS, Van Deventer JSJ, Lukey GC. The characterisation of source materials in fly ash-based geopolymers. Mater Lett 2003;57:1272–80.

[37] Van Deventer JSJ, Provis JL, Duxson P, Lukey GC. Reaction mechanisms in the geopolymeric conversion of inorganic waste to useful products. J Hazard Mater 2007;139:506-13.

[38] Verdolotti L, Iannace S, Lavorgna M, Lamanna R. Geopolymerization reaction to consolidate incoherent pozzolanic soil. J Mater Sci 2008;43:865–73.

[39] Oh JE, Monteiro PJM, Jun SS, Choi S, Clark SM. The evolution of strength and crystalline phases for alkali-activated ground blast furnace slag and fly ash-based geopolymers. Cem Concr Res 2010;40:189–96.

[40] Palomo A, Alonso S, Fernandez-Jiménez A, Sobrados I, Sanz J. Alkaline activation of fly ashes: NMR study of the reaction products. J Am Ceram Soc 2004;87:1141–45.

[41] Fernández-Jiménez A, Palomo A. Composition and microstructure of alkali activated fly ash binder: Effect of the activator. Cem Concr Res 2005;35:1984–92.

[42] Criado M, Fernández-Jiménez A, de la Torre AG, Aranda MAG, Palomo A. An XRD study of the effect of the SiO_2/Na_2O ratio on the alkali activation of fly ash. Cem Concr Res 2007;37:671–79.

[43] Palomo A, Glasser FP. Chemically-bonded cementitious materials based on metakaolin. Br Ceram Trans J 1992;91:107–12.

[44] Temuujin J, Minjigmaa A, Oyun-Erdene G, Davaabal B, Bayarzul U. Characterization of fly ash from "Amgalan" fluidized bed combustion thermal station in Ulaanbaatar city and its applicability for the production of alkali activated material. Fly ash, Nova Science Publishers Inc., New York, 2017;123-35.

[45] Yip CK, Lukey GC, Van Deventer JS. The coexistence of geopolymeric gel and calcium silicate hydrate at the early stage of alkaline activation. Cem Concr Res 2005;35:1688-97.

[46] Provis JL, Bernal SA. Geopolymers and Related Alkali-Activated Materials. Annu Rev Mater Res 2014;44:299–337.

[47] Palomo A, Fernández-Jiménez A, Criado M. "Geopolymers": Same basic chemistry, different microstructures. Mater Constr 2004;54:77–91.